AIP | Review of Scientific Instruments

Multiple pulse-heating experiments with different current to determine total emissivity, heat capacity, and electrical resistivity of electrically conductive materials at high temperatures

Hiromichi Watanabe and Yuichiro Yamashita

Citation: Review of Scientific Instruments **83**, 014904 (2012); doi: 10.1063/1.3680554
View online: http://dx.doi.org/10.1063/1.3680554
View Table of Contents: http://scitation.aip.org/content/aip/journal/rsi/83/1?ver=pdfcov
Published by the AIP Publishing

Multiple pulse-heating experiments with different current to determine total emissivity, heat capacity, and electrical resistivity of electrically conductive materials at high temperatures

Hiromichi Watanabe and Yuichiro Yamashita
Thermophysical Properties Section, Material Properties Division, NMIJ, National Institute of Advanced Industrial Science and Technology, AIST Tsukuba Central 3, 1-1-1, Umezono, Tsukuba, Ibaraki 305-8563, Japan

(Received 8 July 2011; accepted 4 January 2012; published online 31 January 2012)

A modified pulse-heating method is proposed to improve the accuracy of measurement of the hemispherical total emissivity, specific heat capacity, and electrical resistivity of electrically conductive materials at high temperatures. The proposed method is based on the analysis of a series of rapid resistive self-heating experiments on a sample heated at different temperature rates. The method is used to measure the three properties of the IG-110 grade of isotropic graphite at temperatures from 850 to 1800 K. The problem of the extrinsic heating-rate effect, which reduces the accuracy of the measurements, is successfully mitigated by compensating for the generally neglected experimental error associated with the electrical measurands (current and voltage). The results obtained by the proposed method can be validated by the linearity of measured quantities used in the property determinations. The results are in reasonably good agreement with previously published data, which demonstrate the suitability of the proposed method, in particular, to the resistivity and total emissivity measurements. An interesting result is the existence of a minimum in the emissivity of the isotropic graphite at around 1120 K, consistent with the electrical resistivity results. © *2012 American Institute of Physics*. [doi:10.1063/1.3680554]

I. INTRODUCTION

The pulse-heating method[1–3] has been well recognized as an accurate, efficient, and cost-effective method for measuring the specific heat capacity, electrical resistivity, and hemispherical total emissivity of electrically conductive materials at high temperatures. The primary advantage of the pulse-heating method over traditional steady-state methods is the short exposure of the sample to high temperatures, which can reduce contamination of the experimental system and conductive heat loss from the sample. Because of these merits, national measurement institutes in several countries have attempted to apply the pulse-heating method to the establishment of reference materials or recommended data for the heat capacity, electrical resistivity, and emissivity in the high temperature range.[3–7] However, the pulse-heating method still contains a number of drawbacks; two examples of which are discussed here.

One drawback of the pulse-heating method was pointed out by Cezairliyan and co-workers in their measurements of electrical resistivity[5] and specific heat capacity[6] of molybdenum that demonstrates an increase and decrease in the resistivity and heat capacity, respectively, as the sample heating rate is increased in the range below about 4000 K/s. This kind of heating rate effect was also reported for not only molybdenum but also a graphitic material.[1,7] Since the physical properties are intrinsically independent of the heating rate, the heating rate effect indicates the existence of a significant systematic error in the quantities measured in the pulse-heating experiments. Although the most commonly presumed origin of the "extrinsic" heating-rate effect is the systematic error of the sample temperature,[1,5–7] more detailed investigations of the extrinsic effect are required to increase the accuracy of the pulse-heating method.

Another drawback of the pulse-heating method is related to the difficulty in the measurement of the hemispherical total emissivity. In the determination of the emissivity, a basic assumption is that a uniform temperature distribution within the sample is maintained not only during the heating but also subsequent cooling periods. We have reported previously that the measured emissivity could involve severe error due to the rapidly increasing reduction in temperature uniformity within the sample during the cooling period.[8] To solve this problem, the sample itself was used as the resistance thermometer to evaluate the effective temperature of the sample having a nonuniform temperature distribution.[8] However, this method is limited to materials with a resistivity that is monotonically dependent on the temperature. Unfortunately, many electrically conductive materials including isotropic graphite exhibit minimums or maximums in their resistivity-temperature curves.

The objective of the present work is to propose a variant of the pulse-heating method to improve the accuracy in the measurement of the hemispherical total emissivity, specific heat capacity, and electrical resistivity of electrically conductive materials at high temperatures. The proposed method, referred to as the modified pulse-heating method, is applied to a series of pulse-heating experiments on a sample heated at different heating rates and is shown to avoid the extrinsic heating-rate effect by compensation for commonly neglected errors, which are associated with the measurements of the voltage drop along and the current through the sample.

Further, experimental errors due to severe temperature nonuniformity within the sample during the cooling period can be avoided by using only quantities measured during the heating period to determine the three properties. The proposed method is applied to the measurements of the electrical resistivity, specific heat capacity, and hemispherical total emissivity of a commercially available grade of high-density isotropic graphite (IG-110, Toyo Tanso Co. Ltd). IG-110 graphite is recognized as not only an important nuclear grade graphite[9] but is also a thermal diffusivity reference material.[10]

In many pulse-heating experiments, including our previous works[8,11,12] on metals, a division-of-amplitude photopolarimeter[13] (DOAP) was used for *in situ* temperature calibration of the radiation thermometry. However, the surface of graphitic materials tends to be so diffusive that a DOAP cannot be used. Therefore, we adopted a versatile calibration technique based on a combined technique of the transient and brief steady state of the sample.

II. MEASUREMENT PRINCIPLES

A. Conventional pulse-heating method

The conventional pulse-heating method is based on single pulse-heating of an electrically conductive sample from room temperature up to a predetermined high temperature in less than 1 s by the passage of a large current pulse through the sample. In the conventional pulse-heating method, the heating current is switched off to permit the sample to cool down when the sample reaches the preset temperature. Three quantities (the temperature of the sample, the current passing through the sample, and the voltage drop across the sample) are successively measured during the heating and subsequent cooling period to determine the electrical resistivity ρ based on the four-terminal method, the specific heat capacity c_p at constant pressure, and the hemispherical total emissivity ε based on direct heating calorimetry.

Measured values of the voltage drop along and the current through the effective sample ($V_{s,m}$ and I_m, respectively) are used to determine ρ from $\rho = (SV_{s,m})/(LI_m)$ where the effective sample is defined as the partial zone between the pair of voltage probes in contact with the sample surface, and S and L are the cross-sectional area and length of the effective sample, respectively. In addition, I_m is generally calculated to be $V_{r,m}/R_r$ where $V_{r,m}$ is the voltage drop measured across a standard resistor connected in series with the sample and R_r is the nominal standard resistance value. The heat balance of the effective sample having a uniform temperature distribution is expressed in the following equation:

$$mc_p(dT_m/dt) = V_{s,m}I_m - \varepsilon A\sigma_{SB}\left(T_m^4 - T_e^4\right), \tag{1}$$

where m and A are the mass and surface area of the effective sample, respectively, dT_m/dt is the time derivative of the measured sample temperature T_m, σ_{SB} is the Stefan-Boltzmann constant, and T_e is the ambient temperature ($\sim$293 K). By solving a pair of simultaneous equations for the heat balance at a temperature during the heating and subsequent cooling periods of the single pulse-heating experiment, c_p and ε are calculated from

$$c_p = V_{s,m}I_m/[m\{(dT_m/dt)_h - (dT_m/dt)_l\}], \tag{2a}$$

and

$$\varepsilon = V_{s,m}I_m/\left[A\sigma_{SB}\left(T_m^4 - T_e^4\right)\{1 - (dT_m/dt)_h/(dT_m/dt)_l\}\right], \tag{2b}$$

where $(dT_m/dt)_h$ and $(dT_m/dt)_l$ are the respective time derivatives of T_m obtained on heating and cooling.

B. Modified pulse-heating method

In the modified pulse-heating method, the measured quantities $V_{s,m}$, $V_{r,m}$, and T_m are considered to include systematic errors expressed in the following linear relations:

$$V_{s,m} = s_{Vs}V_{s,t} + \Delta V_s, \tag{3a}$$

$$V_{r,m} = s_{Vr}V_{r,t} + \Delta V_r, \tag{3b}$$

$$T_m = s_T T_t + \Delta T, \tag{3c}$$

where $V_{s,t}$, $V_{r,t}$, and T_t are the corresponding true values and (s_{Vs}, s_{Vr}, and s_T) and (ΔV_s, ΔV_r, and ΔT) are the coefficients of the proportional and constant components of the uncertainties of $V_{s,m}$, $V_{r,m}$, and T_m, respectively. Using Eqs. (3a) and (3b), Ohm's law is expressed in the following practical form:

$$V_{s,m} = I_m R_{s,m} + \Delta V_m, \tag{4a}$$

where

$$R_{s,m} = (s_{Vs}/s_{Vr})\,R_{s,t}, \tag{4b}$$

$$\Delta V_m = \Delta V_s - \left(R_{s,m}/R_r\right)\Delta V_r, \tag{4c}$$

and where $R_{s,t}$ is the true value of the effective sample electrical resistance. To determine $R_{s,m}$ at a temperature, rapid resistive self-heating of the sample from room temperature to a high temperature above the target temperature is repeated more than three times and the heating current preset level is changed for each experiment. From Eq. (4a), $R_{s,m}$ can be determined as the slope of the linear least-squares fit for the measured multiple (I_m, $V_{s,m}$) values. The determinable value of $R_{s,m}$ can be regarded as $R_{s,t}$, because both s_{Vs} and s_{Vr} are generally assumed to be unity based on sufficient calibration of the device for measuring the voltage drop. Therefore, the electrical resistivity is calculated from $\rho \approx \rho_m = (S/L)R_{s,m}$. Since $V_{s,m}$ and $V_{r,m}$ are measured simultaneously by the same device, we can assume that both ΔV_s and ΔV_r exhibit an identical magnitude ΔV. In this case, the sample heat balance equation expressed by Eq. (1) can be rewritten as follows:

$$Y = c_{p,m}X + \varepsilon_m, \tag{5a}$$

where

$$Y = \frac{(V_{s,m} - \Delta V)(V_{r,m} - \Delta V)}{R_r A\sigma_{SB}\left(T_m^4 - T_e^4\right)}, \tag{5b}$$

$$X = \frac{m(dT_m/dt)}{A\sigma_{SB}\left(T_m^4 - T_e^4\right)}, \tag{5c}$$

$$c_{p,m} = (s_{Vs}s_{Vr}s_T)c_p, \tag{5d}$$

$$\varepsilon_m = \left(s_{Vs}s_{Vr}\frac{T_t^4 - T_e^4}{T_m^4 - T_e^4}\right)\varepsilon \approx \left(s_{Vs}s_{Vr}s_T^{-4}\right)\varepsilon, \tag{5e}$$

$$\Delta V = \Delta V_m/(1 - R_{s,m}/R_r), \tag{5f}$$

and where the approximation in Eq. (5e) holds in the common case that T_m is much greater than each of T_e and ΔT. By using Eq. (5f), the value of ΔV can be calculated fromΔV_m, which can be determined from the intercept of the least-squares linear fit of the multiple (I_m, $V_{s,m}$) data sets. Since X and Y are measurable quantities, $c_{p,m}$ and ε_m can be determined similarly by the respective slope and intercept of the linear fit obtained by the least-squares method on multiple (X, Y) data sets measured at different heating rates. The determinable values of $c_{p,m}$ and ε_m are regarded as the target values of c_p and ε, respectively, because s_T can also be regarded to be unity.

III. EXPERIMENTS AND UNCERTAINTY ESTIMATION

A. Experimental setup

The experimental setup used in this work consisted of a vacuum chamber containing the sample, an electrical pulse-heating circuit, a radiation thermometer, and a computer system for the data acquisition and process control. A schematic diagram of the setup is shown in Fig. 1. The IG-110 graphite sample was cut into a plate ~4 mm wide, 40 mm long, and 0.5 mm thick. The bulk density and surface roughness of the sample at room temperature (~293 K) were measured to be 1.7819 g/cm^3 and 1.506 μm, respectively. The sample was connected in series with heavy-duty batteries, a standard resistor (15 mΩ) for measuring the current, and field effect transistors (FETs) for regulating the current level. A pair of knife-edge probes made of tungsten was spring loaded onto the sample surface to measure the voltage drop across the effective sample ($S = 1.9710$ mm^2 and $L = 18.983$ mm). The radiance temperature of a circular area (1 mm in diameter) at the center of the rectangular sample surface (40 × 4 mm^2) was measured using the radiation thermometer that had a detecting wavelength range of 1.58–1.8 μm (model: KG740, KLEIBER Infrared GmbH). The radiance temperature and voltage drops across the sample and standard resistor were recorded every 5 μs by a 14-bit simultaneous sampling data-acquisition device (model: PXI-6133, National Instruments) included in the computer system. The sample was repeatedly heated up to ~1850 K at six different heating rates. All six pulse-heating experiments were conducted in vacuum below 5×10^{-4} Pa.

The response time of the radiation thermometer (~6 μs) was short enough to follow the sample heating rate (1800–6000 K/s) realized in this work. To determine the true temperature of the sample, an R type thermocouple 50 μm in diameter was attached with a carbon adhesive at the center of the sample surface, the back side of which was the target area of the radiation thermometer. However, the response of the thermocouple could not match the temperature variation during the heating period. Therefore, a fitted polynomial function was used to calculate the true temperature from the radiance temperature. The coefficients of the fitted polynomial were determined by combined transient and steady-state experiments.

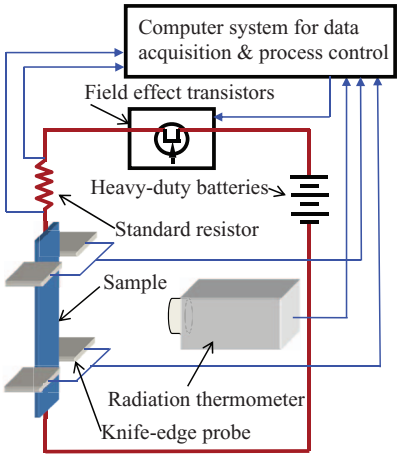

FIG. 1. (Color online) Schematic diagram of the experimental setup.

B. Temperature calibration

Figure 2 shows a typical example of the respective time evolutions of the radiance temperature T_a and the electromotive force *emf* of the thermocouple while the sample was heated and then maintained at a constant temperature and finally cooled down. This figure shows that T_a was controlled to follow three stages:

(1) T_a rapidly increases up to the preset value $T_{a,p}$,
(2) T_a is maintained at $T_{a,p}$ for a brief period, and
(3) T_a decreases from $T_{a,p}$.

During the first stage ($t < 205$ ms), the gate voltage of the FETs that controls the current passing through the sample was kept at a high level to increase T_a up to $T_{a,p}$ at a heating rate above 1500 K/s. In the second stage (205 ms $\leq t \leq$ 1143 ms) the gate voltage was feedback controlled at 10 kHz to maintain T_a at $T_{a,p}$ from $t = 205$–1103 ms, and then, was held at the average temperature of the last 100 values for $t = 1103$–1143 ms as computed by a feedback-control proportional integral derivative algorithm. During the third stage, the gate

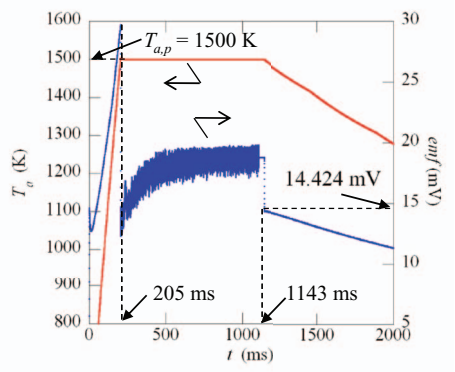

FIG. 2. (Color online) Results of the radiance temperature T_a and electromotive force *emf* of the thermocouple as a function of time in the rapid calibration of the radiance thermometer.

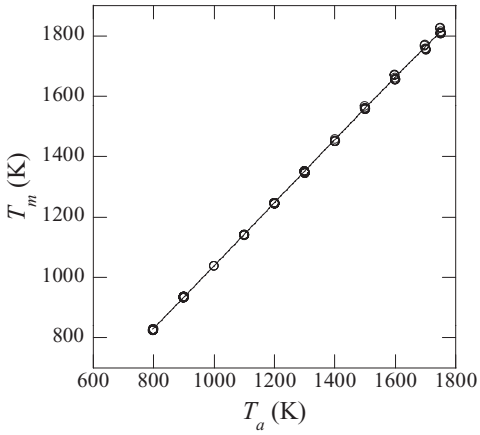

FIG. 3. Results of the temperature T_m as a function of T_a for the IG-110 graphite sample.

voltage was reset to zero to stop supplying current. It should be noted that the measured *emf* includes a voltage-drop error due to the current passing through the thermocouple junction during the first and second stages. The sharp decrease of the *emf* at the beginning of the second stage (205 ms) is a result of the reduction of the current through the junction. On the other hand, the gradual increase of the *emf* after the sharp decrease indicates that the thermocouple could not attain thermal equilibrium with the sample during the initial part of the second stage. The temperature of the sample is required to be determined after the attainment of the thermally equilibrium state. Therefore, the temperature (1558.6 K) calculated from the measured *emf* (14.424 mV) at the beginning of the third stage was regarded as the true value when the radiance temperature was $T_{a,p}$ (1500 K). The feedback control caused the severe noise in the *emf*, which is illustrated in the time region from 205 ms to 1103 ms (Fig. 2). To minimize the additional error in the *emf*, the feedback control of the gate voltage was halted 40 ms before the second-stage end time. The rapid calibration process was realized by the installation of a real-time operating system into the feedback-control program originally developed by Matsumoto and Cezairliyan,[14] and was repeated for different $T_{a,p}$ temperatures to determine the temperature T_m as a function of T_a. The plot shown in Fig. 3 was obtained from three hundred simultaneous measurement results of T_a and the *emf* at eleven values of $T_{a,p}$ for the IG-110 graphite sample. The solid line represents the third-order polynomial for computing T_m as a function of T_a, which is fitted to all independent pairs (T_m, T_a) by a least-squares method. After accomplishing the calibration for the whole temperature range of interest, the thermocouple was removed from the sample surface to avoid any influence on the main measurements.

C. Evaluation of expanded uncertainty

In order to validate the performance of the modified pulse-heating method, the expanded uncertainties of the three measured properties were determined based on the following well-accepted equation:

$$U(z) = k_{95}(v_{eff})u_c(z), \tag{6}$$

where $U(z)$ is the expanded uncertainty of an estimated quantity z, $k_{95}(v_{eff})$ is a coverage factor providing a level of confidence of approximately 95% with a basis on the t-distribution for v_{eff} that is the effective degrees of freedom estimated from the Welch-Satterthwaite formula, and $u_c(z)$ is the combined standard uncertainty. The present values of $u_c(z)$ and v_{eff} for each the three results were estimated as described below.

On the assumption that $s_{Vs} = s_{Vr} = s_T = 1$, the combined standard uncertainties of ρ, c_p, and ε can be evaluated from the following equations:

$$\frac{u_c^2(\rho)}{\rho_m^2} = \frac{u^2(\rho_m)}{\rho_m^2} + u^2(s_{Vs}) + u^2(s_{Vr}) + \left(\frac{d\rho_m}{dT_m}\right)^2 \frac{u^2(T_m)}{\rho_m^2}, \tag{7a}$$

$$\frac{u_c^2(c_p)}{c_{p,m}^2} = \frac{u^2(c_{p,m})}{c_{p,m}^2} + u^2(s_{Vs}) + u^2(s_{Vr}) + u^2(s_T) + \left(\frac{dc_p}{dT_m}\right)^2 \frac{u^2(T_m)}{c_{p,m}^2}, \tag{7b}$$

$$\frac{u_c^2(\varepsilon)}{\varepsilon_m^2} = \frac{u^2(\varepsilon_m)}{\varepsilon_m^2} + u^2(s_{Vs}) + u^2(s_{Vr}) + 16u^2(s_T) + \left(\frac{d\varepsilon_m}{dT_m}\right)^2 \frac{u^2(T_m)}{\varepsilon_m^2}, \tag{7c}$$

where $u(x)$ and dx/dT_m represent the standard uncertainty and temperature derivative of the quantity x, respectively. The final terms in Eqs. (7a)–(7c) are added to take into account the temperature dependence of ρ, c_p, and ε, respectively. The temperature derivatives were estimated from the measured results. The systematic error caused by the thermal expansion of the sample was compensated for using the high-temperature sample dimensions estimated from the manufacturer's catalogue data[15] for the linear thermal expansion of IG-11 graphite, which is the most similar grade to IG-110.

Values of $u(\rho_m)$ and $u(c_{p,m})$ were calculated from the well-known standard uncertainty expression of the slope of the linear least-squares fit ($y = \alpha x + \beta$) on a set of n pairs (x, y) as follows:

$$u(\alpha) = \sqrt{\frac{\sum_{i=1}^{n}\{y_i - (\beta x_i + \alpha)\}^2}{(n-2)\sum_{i=1}^{n}(x_i - \overline{x})^2}}, \tag{8}$$

where $\overline{x}$ represents the arithmetic mean of the n independent values of x. The multiple data sets for (I_m, $V_{s,m}$) and (X, Y) were substituted for the n pairs (x, y) in Eq. (8) to determine $u(\rho_m)$ and $u(c_{p,m})$, respectively. On the other hand, $u(\varepsilon_m)$ was estimated as the standard uncertainty of the intercept of the linear least-squares fit of (X, Y) as follows:

$$u(\varepsilon_m) = \sqrt{\frac{\sum_{i=1}^{n}\{Y_i - (c_{p,m}X_i + \varepsilon_m)\}^2}{(n-2)}\left\{\frac{1}{n} + \frac{\overline{X}^2}{\sum_{i=1}^{n}(X_i - \overline{X})^2}\right\}}, \quad (9)$$

where $\overline{X}$ represents the arithmetic mean of the n independent values of X.

The magnitude of $u(s_T)$ was estimated to be 0.46% from the respective inaccuracies of the radiation thermometer (0.75%) and thermocouple (0.25%) used in this work on the assumption that both the probability distributions are rectangular. From Eq. (3c), the magnitude of $u(T_m)$ was calculated from the following equation:

$$u(T_m) = \sqrt{u^2(s_T)\,T_m^2 + \Delta T^2}. \quad (10)$$

The magnitude of ΔT was estimated to be 0.30 K from the experimental standard deviation of the fitted curve shown as the solid line in Fig. 3.

Due to the similarity of the measurements of $V_{s,m}$ and $V_{r,m}$, we can consider $u(s_{Vs})$ to be identical to that of $u(s_{Vr})$. The common uncertainty was estimated to be 305 ppm from the specification data on the gain error (226 ppm), offset error (208 ppm), and one-year instability (429 ppm) of the data-acquisition device, on the assumption that their probability distributions are rectangular.

IV. RESULTS AND DISCUSSION

A. Extrinsic heating-rate effect

To investigate the extrinsic heating-rate effect, the electrical resistivity results obtained under the different heating-rate conditions are compared. The temperature-time curves shown in Fig. 4(a) were obtained in the six independent pulse-heating experiments where the current through the IG-110 sample was set at the different levels shown in the figure, and the resistivity-temperature curves shown in Fig. 4(b) were obtained from the same six experiments. The values of the resistivity were calculated from $\rho = (SV_{s,m})/(LI_m)$, which considers no correction for the voltage-drop error. An inspection of Fig. 4(b) indicates that the resistivity increases with the heating rate (current) over the entire measured temperature range.

The extrinsic heating-rate effect on the pulse-heating experiment is generally considered to be due to temperature nonuniformity within the sample. When a sample heats at a low rate, temperature gradients are established in the axial direction due to heat conduction from the sample to the sample holders placed at the sample ends. As a result, the average temperature of the effective sample will be lower than the measured temperature corresponding to the sample midpoint temperature. This will tend to lower the computed values of the measured property with respect to that determined under conditions of uniform temperature if it has a positive temperature coefficient. However, the electrical resistivity of IG-110 exhibits a minimum at ~1060 K. Therefore, the positive heating-rate coefficient of the resistivity at temperatures below 1060 K cannot be explained in terms of the nonuniform temperature distribution.

The other possible error causing the extrinsic heating-rate effect is the error in voltage-drop measurements. From Eqs. 4(a)–4(c), the electrical resistivity ρ_s obtained by the conventional pulse heating method, which is independent of the voltage-drop error, is given by

$$\rho_s\left(=\frac{SV_{s,m}}{LI_m}\right) = \left(\frac{s_{Vs}}{s_{Vr}}\right)\rho + \frac{S\{\Delta V_s - (R_{s,m}/R_r)\Delta V_r\}}{LI_m}. \quad (11)$$

Equation (11) indicates that ρ_s is inversely proportional to I_m. Namely, ρ_s depends on the heating rate of the sample. Therefore, the systematically positive dependence of the resistivity on the heating rate, as shown in Fig. 4, can occur if the sign of the second term in Eq. (11) is negative. Therefore, we conclude that the constant components of the voltage-drop error can cause the extrinsic heating-rate effect on the resistivity measurements.

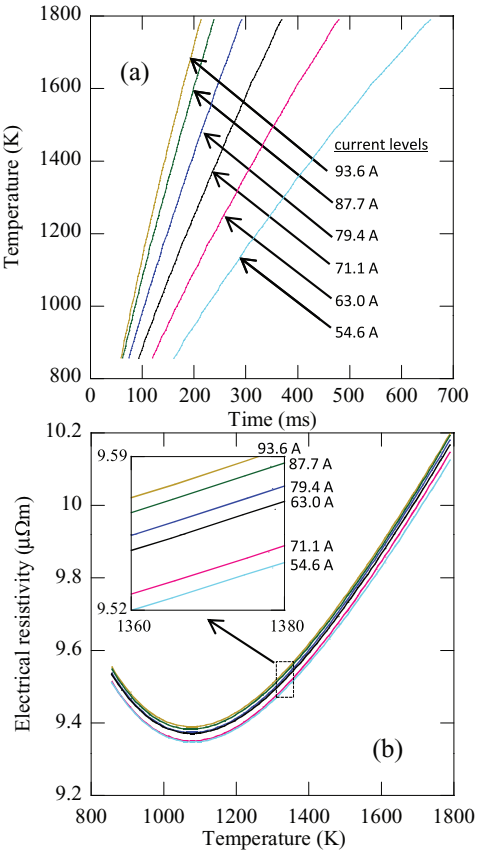

FIG. 4. (Color online) Results of (a) the radiance temperature as a function of time and (b) the electrical resistivity evaluated without the correction of the voltage drops as a function of temperature, both of which were obtained in a set of repeated pulse-heating experiments on the IG-110 graphite sample heated at six different heating rates by adjusting the preset current level.

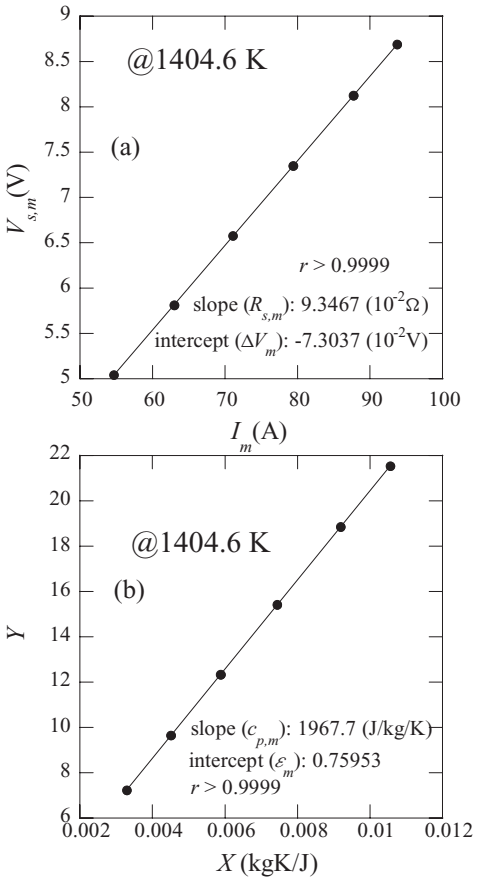

FIG. 5. The pair plots of (a) (I_m, $V_{s,m}$) and (b) (X, Y) for the IG-110 graphite sample at 1404.6 K in the six independent experiments shown in Fig. 4. The linearity of the plots demonstrates the validity of the modified pulse-heating method.

B. Linearity of the voltage-current and newly adopted *X*–*Y* relationships

To estimate the applicability of the modified pulse-heating method, both the linearity of the measured voltage-current and X–Y relationships need to be verified. As an example, the pair plots ($V_{s,m}$–I_m and X–Y) obtained at 1404.6 K in the six pulse-heating experiments are shown in Figs. 5(a) and 5(b), respectively. The solid lines in the figures represent the linear least-squares fits, and demonstrate the good linearity of both of the relationships. All the correlation coefficients for the linear fits at the temperatures investigated were greater than 0.999. By substituting the measured ΔV_m (-7.3037×10^{-2} V) into Eq. (5f), the constant component of the voltage-drop error, i.e., ΔV, was estimated to be -1.3962×10^{-2} V. In this work, all the measured values of ΔV, which were scattered over the range between -18 and -10 mV, were beyond the inaccuracy of the device used in the voltage measurement. These results confirm that the modified pulse-heating method is applicable and suitable to the measurements of the three properties for IG-110 graphite.

C. Resistivity, heat capacity, and total emissivity by modified pulse-heating method

Results of the electrical resistivity, specific heat capacity, and hemispherical total emissivity of IG-110 as a function of temperature measured by the modified pulse-heating method are shown in Figs. 6(a)–6(c), respectively. The solid circles and uncertainty bars in the three figures represent the present results and expanded uncertainties of IG-110 graphite, respectively. For the emissivity results, there is a lack of data below 1000 K due to the large value of $\varepsilon + U(\varepsilon)$, which was beyond the permissible level, i.e., unity. The relatively large uncertainty observed around the lower, and also upper limits, of the measured range was caused by the significantly large value of $u(\varepsilon_m)$. The lines associated with the circles correspond to the least-squares polynomial fits of the IG-110 property results as a function of temperature. An interesting result for the total emissivity is the existence of a minimum at around 1120 K,

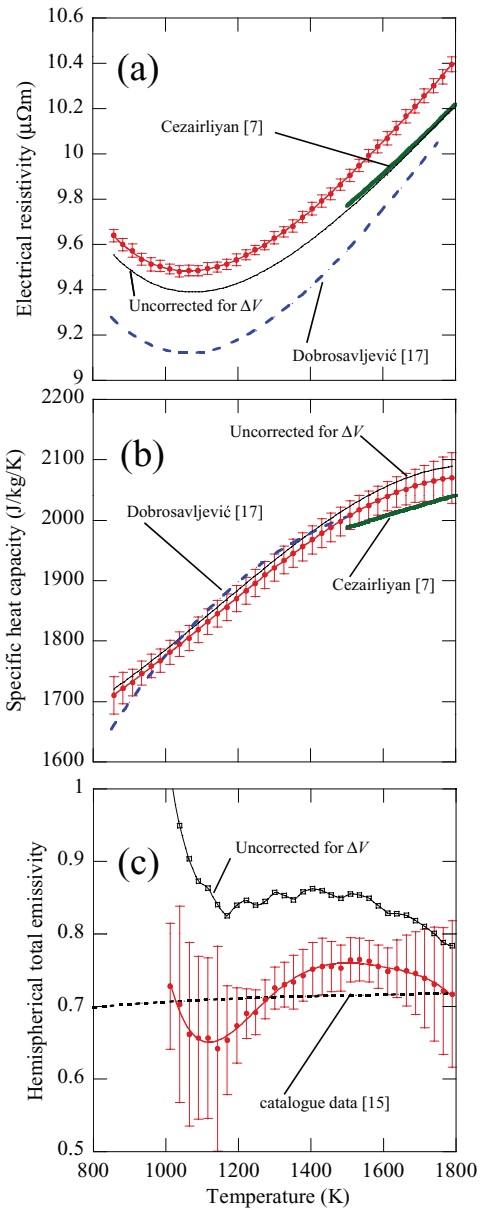

FIG. 6. (Color online) Results of temperature dependence of (a) electrical resistivity, (b) specific heat capacity, and (c) hemispherical total emissivity of IG-110 graphite, together with the data from the literature for the resistivity and heat capacity of POCO AXM-5Q1 graphite, the catalogue data of the emissivity of IG-610U graphite, and the three property results uncorrected for the voltage-drop error.

consistent with the electrical resistivity results which display a minimum at almost the same temperature. This similarity implies that the total emissivity of IG-110 is correlated with the electrical resistivity; the relationship between the emissivity and resistivity of metals is explained by the Hagen-Rubens relation or its modified theoretical models.[16]

From an analytical point of view, the difference between the modified and conventional pulse-heating methods is whether or not the correction for ΔV is taken into account. To evaluate the influence of ΔV on the measured results, re-evaluated property results under the assumption that ΔV can be neglected are compared with the present results in Figs. 6(a)–6(c). The uncorrected resistivity-temperature curve in Fig. 6(a) is identical to the curve in Fig. 4(b) that corresponds to the experiment where the current level was set to the maximum value (93.6 A). For the heat capacity and total emissivity, the uncorrected results are obtained by the modified pulse-heating method from the six experiments, although ΔV is regarded to be zero. As shown in Figs. 6(a) and 6(c), there exist significant discrepancies between the corrected and uncorrected results for the resistivity and total emissivity. On the other hand, the uncorrected and corrected heat capacity results are in agreement with the expanded uncertainty. As a result, the resistivity and total emissivity measurements are affected by the voltage-drop error, while the heat capacity is not.

D. Comparison with published work

The present results are compared with published data of the resistivity and heat capacity for POCO AXM-5Q1 graphite measured by Cezairliyan and Miiller,[7] Dobrosavljević *et al.*,[17] and the catalogue data[15] of the total emissivity of IG-610U graphite, as shown in Fig. 6. Although the measured resistivity of IG-110 is greater than both sets of data previously published for POCO AXM-5Q1, the measured heat capacity agrees well with both the heat capacity data on POCO AXM-5Q1. The total emissivity results on IG-110 are also in good agreement with the emissivity data on IG-610U. Both POCO AXM-5Q1 and IG-610U are categorized as the high-density isotropic graphitic materials including IG-110, and the former is a world-wide standard material for the category, while the later is a similar grade produced by the manufacturer of IG-110. The resistivity and heat capacity values for POCO AXM-5Q1 were determined by the conventional pulse-heating method, and the IG-610U emissivity data were based on the direct comparison with the blackbody radiation.

For the electrical resistivity, the relative differences between the present and published results are estimated to be −1.2 and −3.9%. The resistivity discrepancy is considered to be partially due to the voltage-drop correction adopted in the present work. In the work of Cezairliyan and Miiller,[7] the extrinsic heating-rate effect was observed; the measured resistivity of POCO AXM-5Q1 increased with the sample heating rate over a range below about 2000 K/s. This could suggest the existence of significant voltage-drop error in the experimental work. In addition, the thermal expansion compensation adopted in the present work is also associated with the discrepancy. Contrary to the present results, the data from the literature were calculated using the geometrical quantities of the samples at room temperatures. The effect of thermal expansion compensation for IG-110 causes the estimated resistivity to increase from 0.24 to 0.81% as the temperature increases from 800 to 1800 K. Although the bulk density of the IG-110 is greater than that of the POCO AXM-5Q1 by 1 to 2%, the density difference may not be significantly related to the resistivity discrepancy, because the resistivity generally decreases with increasing density in isotropic graphitic materials.

For the heat capacity, the measurement is insensitive to the voltage-drop error, as described in Sec. IV C. We can consider that the insensitivity contributes to the relatively good agreement with the published heat capacity data[7,17] on POCO AXM-5Q1. In fact, the heat capacity results obtained by Cezairliyan and Miiller[7] also indicate an insensitivity to the voltage-drop error. They reported that the measured heat capacity was independent of the heating rate but the simultaneously measured resistivity increased with the heating rate. This difference in sensitivity of the resistivity and heat capacity to the heating rate is very similar to that observed in the present work.

For the total emissivity, the agreement with the emissivity data[15] on IG-610U ensures the validity of the modified pulse-heating method, because the IG-610U data were measured based on a quite different measurement principle. Further, it may be stated here that no total emissivity data for POCO AXM-5Q1 were reported in published pulse-heating experimental works,[7,17] although the conventional pulse-heating method yields not only the resistivity and heat capacity but also the total emissivity. The reason for the absence of the emissivity data may be due to the voltage-drop error that is generally ignored or the possible severe nonuniformity of the temperature distribution within the cooling sample in the conventional method.

Some technical differences, especially for the thermometry, also may contribute to the discrepancy between the present and published results. In the present work, the radiation thermometry calibration using the comparison with contact thermometry was carried out during the brief thermal steady state between the sample and thermocouple in contrast to the previous calibration in the study of Dobrosavljević *et al.*[17] In the study of Cezairliyan and Miiller,[7] only the radiation thermometer was used to measure the temperature of the sample in the form of a cylindrical tube. A small rectangular hole was fabricated at the middle of the sample tube and was used as a blackbody cavity for the radiation thermometry. Kaschnits and Supancic[18] have pointed out that the existence of such a blackbody hole unavoidably disturbs the temperature and current density distributions within the sample on the basis of three-dimensional finite-element analysis.

V. CONCLUSIONS

A methodology for analytical and experimental procedures of a modified pulse-heating method has been presented. The electrical resistivity, specific heat capacity, and

hemispherical total emissivity of IG-110 graphite have been determined by the multiple pulse-heating experiments with different current. The two problems of extrinsic heating-rate effect and nonuniform temperature distribution within the cooling sample, both of which are sources of error in the conventional pulse-heating method, have been successfully avoided by compensating for the generally neglected voltage-drop error and by applying only the measured quantities of the heated sample analytically, respectively. The combined technique of transient and brief steady-state experiments is adopted to minimize the temperature error associated with the relatively slow response of the contact thermometry. The property results are self-validated based on both the linearity of the measured voltage-current and newly adopted $X-Y$ relationships. The present results are in reasonably good agreement with previously published data, although the difference in the resistivity cannot be explained sufficiently. In conclusion, the present work demonstrates that the modified pulse-heating method can increase the accuracy in property measurements at high temperatures.

ACKNOWLEDGMENTS

This study was financially supported by the Industrial Technology Research Grant Program (Project No. 09A28003a) of the New Energy and Industrial Technology Development Organization (NEDO).

[1]A. Cezairliyan, in *Compendium of Thermophysical Property Measurement Methods*, edited by K. D. Maglić, A. Cezairliyan, and V. E. Peletskii (Plenum, New York, 1992), Vol. 2, p. 483.
[2]K. D. Maglić and A. S. Dobrosavljević, Int. J. Thermophys. **13**(1), 3 (1992).
[3]F. Righini, G. C. Bussolino, and J. Spišiak, Thermochim. Acta **347**(1–2), 93 (2000).
[4]K. D. Maglić, Int. J. Thermophys. **24**(2), 489 (2003).
[5]A. Cezairliyan, Int. J. Thermophys. **1**(4), 417 (1980).
[6]A. Cezairliyan, Int. J. Thermophys. **4**(2), 159 (1983).
[7]A. Cezairliyan and A. P. Miiller, Int. J. Thermophys. **6**(3), 285 (1985).
[8]H. Watanabe and T. Matsumoto, Rev. Sci. Instrum. **76**(4), 043904 (2005).
[9]I. Masahiro, S. Junya, S. Taiju, I. Tatsuo, and O. Tatsuo, Nucl. Eng. Des. **233**(1–3), 251 (2004).
[10]M. Akoshima and T. Baba, Int. J. Thermophys. **26**(1), 151 (2005).
[11]H. Watanabe, Rev. Sci. Instrum. **77**(3), 036110 (2006).
[12]H. Watanabe and T. Baba, Appl. Phys. Lett. **88**(24), 241901 (2006).
[13]S. Krishnan, J. Opt. Soc. Am. A **9**(9), 1615 (1992).
[14]T. Matsumoto and A. Cezairliyan, Int. J. Thermophys. **18**(6), 1539 (1997).
[15]See www.toyotanso.co.jp/Products/Pdf/Special-Compound_e.pdf.
[16]A. J. Sievers, J. Opt. Soc. Am. **68**(11), 1505 (1978).
[17]A. Dobrosavljević, N. Perović, and K. Maglić, High Temp. - High Press. **19**, 303 (1987).
[18]E. Kaschnitz and P. Supancic, Int. J. Thermophys. **26**(4), 957 (2005).